MODELING TIME-VARYING REACTANCES USING WAVE DIGITAL FILTERS

Ólafur Bogason

Genki Instruments
Reykjavik, Iceland
olafur@genkiinstruments.com

Kurt James Werner

The Sonic Arts Research Centre (SARC)
School of Arts, English and Languages
Queen's University Belfast, UK
k.werner@qub.ac.uk

ABSTRACT

Wave Digital Filters were developed to discretize linear time invariant lumped systems, particularly electronic circuits. The time-invariant assumption is baked into the underlying theory and becomes problematic when simulating audio circuits that are by nature time-varying. We present extensions to WDF theory that incorporate proper numerical schemes, allowing for the accurate simulation of time-varying systems.

We present generalized continuous-time models of reactive components that encapsulate the time-varying lossless models presented by Fettweis, the circuit-theoretic time-varying models, as well as traditional LTI models as special cases. Models of time-varying reactive components are valuable tools to have when modeling circuits containing variable capacitors or inductors or electrical devices such as condenser microphones. A power metric is derived and the model is discretized using the alpha-transform numerical scheme and parametric wave definition.

Case studies of circuits containing time-varying resistance and capacitance are presented and help to validate the proposed generalized continuous-time model and discretization.

1. INTRODUCTION

Time-varying lumped systems involve at least one parameter, e.g. the value of a resistor, that is changed over time. Many musical circuits are time-varying, including auto-wah pedals, phasers, and indeed most every circuit where a user can twist a knob on the fly. Some circuits may involve time-varying reactances, for instance ladder filters with variable inductors or stepped filters where reactances may be switched in and out. In virtual analog, stability and energy-preservation under time-varying conditions has been studied in, e.g., [1, 2, 3]. However in certain electrical devices, e.g. condenser microphones, the *dynamics* of a time-varying reactance (in that case, a capacitor) are the main operating principle of the device and the system may not actually be energy-preserving under time-varying conditions in continuous time. In virtual analog, modeling time-varying reactances is essential, both to accurately simulate time-varying phenomena in electrical systems and to develop principles for time-varying digital filters based on static analog filters, e.g. adaptive digital filtering.

Wave Digital Filters (WDFs) provide a computationally efficient way to simulate lumped element models [4] with excellent numerical properties. Recent developments in the field include topological advances in linear and nonlinear circuits [5, 6, 7], the introduction of new wave variable definitions, including parametric waves [8] and bi-parametric waves [9] and the development of new discretization schemes [10] applied to WDFs [8, 11, 12]. In the WDF literature there has been some research done on time-varying systems. By giving up guaranteed stability, Strube ex-

tended the paradigm to two dimensions to model vocal tracts [13, 14]. Stability of passive, time-varying circuits [15, 16] has been proven for WDF algorithms that employ power-normalized waves as signal variables and guaranteed stable approaches to varying the step-size on the fly have also been studied [17, 18].

The paper is structured as follows. In the rest of this section, we discuss notation and background information. In §2 we discuss continuous-time models of capacitors and inductors and propose novel generalized models of these reactances. In §3 we discuss discretization schemes for reactances in the WDF paradigm and discretize the generalized models. We use the newly discretized model to study the effects of time-varying resistance (§4) and reactance (§5) on the dc response of a RC circuit. §6 presents recommendations for time-varying WDF simulations and concludes.

1.1. Wave Variables

Instead of the Kirchhoff signal variables from circuit theory, voltage v and current i, in WDFs the *wave*-variables, a and b for incident and reflected waves, are used [4]. The parametric wave definition is a useful tool that was recently introduced [7, 8] as a parametrization of the traditional wave-variables. At port 0 in a circuit a linear transformation from the Kirchhoff domain $\mathcal{K}$ to the Wave-domain $\mathcal{W}$ is defined as

$$\begin{bmatrix} a_0 \\ b_0 \end{bmatrix} = R_0^\rho \begin{bmatrix} R_0^{-1} & 1 \\ R_0^{-1} & -1 \end{bmatrix} \begin{bmatrix} v_0 \\ i_0 \end{bmatrix} = \mathbf{\Phi}_{\mathcal{KW}} \begin{bmatrix} v_0 \\ i_0 \end{bmatrix}. \tag{1}$$

When $\det(\mathbf{\Phi}_{\mathcal{KW}}) = -2R_0^{2\rho-1} \neq 0$ (i.e. $R_0 \neq 0$), the inverse is

$$\begin{bmatrix} v_0 \\ i_0 \end{bmatrix} = \frac{1}{2} R_0^{-\rho} \begin{bmatrix} R_0 & R_0 \\ 1 & -1 \end{bmatrix} \begin{bmatrix} a_0 \\ b_0 \end{bmatrix} = \mathbf{\Phi}_{\mathcal{WK}} \begin{bmatrix} a_0 \\ b_0 \end{bmatrix}. \tag{2}$$

Note that $\mathbf{\Phi}_{\mathcal{WK}}\mathbf{\Phi}_{\mathcal{KW}} = \mathbf{\Phi}_{\mathcal{KW}}\mathbf{\Phi}_{\mathcal{WK}} = \mathbf{I}$ irrespective of the value of ρ, where $\mathbf{I}$ is the identity matrix. By varying the real parameter ρ, a family of transforms that include the standard voltage, power-normalized and current waves may be obtained

$$\rho \triangleq \begin{cases} 1 & \text{voltage waves} \\ 1/2 & \text{power-normalized waves} \\ 0 & \text{current waves} \end{cases}. \tag{3}$$

Plugging the definition (2) into the definition $p_0 = v_0\, i_0$ of instantaneous power at a port 0 gives the wave-domain power

$$p_0 = \frac{1}{4} R_0^{1-2\rho}(a_0^2 - b_0^2). \tag{4}$$

Note that the expression becomes independent of the port resistance when power-normalized waves are used ($\rho = 1/2$) [15].
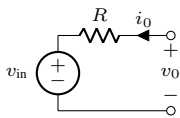
Figure 1: *Res. v. source.*

Table 1: *Source WDF mults.*

Adapted?	f	g
No	$\frac{R-R_0}{R+R_0}$	$\frac{2R_0^\rho}{R+R_0}$
$R_0 = R$	0	$R^{\rho-1}$

(a) *Unadapted resistive source.* (b) *Adapted resistive source.*

Figure 2: *WDF signal flow graphs for resistive sources.*

1.2. Resistive Voltage Source Derivation

As an example of how to derive wave-domain equations using the parametric wave definition, consider the resistive voltage source (Fig. 1). In the Kirchhoff domain, its constitutive equation is

$$v_{\text{in}} = v_0 - R\,i_0\,, \qquad (5)$$

where v_{in} is the voltage source value and R is the resistor's value. Since this source represent an instantaneous geometric relationship, time indices in continuous and discrete time are suppressed.

Plugging in the parametric wave definition (2) and solving for b_0 yields the unadapted wave-domain equation

$$b_0 = \frac{R-R_0}{R+R_0}a_0 + \frac{2R_0^\rho}{R+R_0}v_{\text{in}}\,. \qquad (6)$$

This wave-domain equation is adapted by setting $R_0 = R$, yielding the adapted wave-domain equation

$$b_0 = R^{\rho-1}v_{\text{in}}\,. \qquad (7)$$

Note that ρ does not affect the adaptation criteria or reflectance (multiplication of incident wave a_0) but rather only contributes to scaling the input v_{in} [15, 8].

In the rest of the paper, we will need to refer directly to the adapted and unadapted multipliers in the resistive voltage source. To enable this we will define a generic wave-domain equation

$$b_0 = f\,a_0 + g\,v_{\text{in}}\,, \qquad (8)$$

where f is the reflectance and g is the input scaling. These values are defined for unadapted and adapted resistive voltage sources in Tab. 1. The corresponding signal flow graphs are given in Fig. 2. Here triangles represent multiplications, $+$ symbols represent addition, unfilled semicircles represent wave sources, filled semicircles represent wave sinks. Throughout the paper a shaded background indicates that an element is the root of a WDF tree.
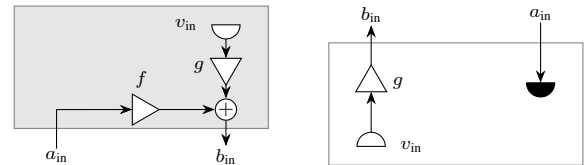
A full review of WDF elements defined with the parametric wave definition is beyond the scope of this paper. The reader is referred to [8] for a full catalog of WDF elements.

1.3. First-Order Difference Equation

In this paper we use multiplication coefficients of a first-order difference equation to show how parameters from continuous-time models, discretization schemes and the choice of wave-variables influence the WDF difference equation for reactive elements. We chose a difference equation of common form [19] and notate coefficients as d_1, n_0 and n_1 (d for "denominator" and n for "numerator") rather than the more common a and b to avoid confusion with wave variable notation [20]

$$b_0[n] = -d_1\,b_0[n-1] + n_0\,a_0[n] + n_1\,a_0[n-1]\,. \qquad (9)$$

We use direct-form I [19] filter topologies in all realizations.

2. MODELING REACTIVE COMPONENTS

Here we review continuous-time capacitor and inductor models, including traditional LTI models, models proposed by Fettweis, and models used for time-varying components. Noting that they differ only in terms of which quantities are differentiated, we propose novel generalized continuous-time capacitor and inductor models that include the previous three models as special cases.

2.1. Models from Traditional WDF Theory

In traditional WDF theory [4], which is based on classical circuit theory, reactive elements were modeled as ideal. The constitutive equations for these elements are

$$i(t) = C(t)\frac{\mathrm{d}v(t)}{\mathrm{d}t}\,, \quad (10) \qquad v(t) = L(t)\frac{\mathrm{d}i(t)}{\mathrm{d}t}\,, \quad (11)$$

where C is the capacitor's capacitance in Farads (F) and L is the inductor's inductance in Henries (H).

2.2. Fettweis' Lossless Models

In [21], Fettweis proposed following time-varying models

$$i(t) = \sqrt{C(t)}\,\frac{\mathrm{d}}{\mathrm{d}t}\left(\sqrt{C(t)}\,v(t)\right), \qquad (12)$$

$$v(t) = \sqrt{L(t)}\,\frac{\mathrm{d}}{\mathrm{d}t}\left(\sqrt{L(t)}\,i(t)\right), \qquad (13)$$

for a capacitor and inductor respectively. These models are lossless [16] as will be shown in §2.4.

2.3. Models from Circuit Theory

In circuit theory time-varying reactive models are given by

$$i(t) = \frac{\mathrm{d}q(t)}{\mathrm{d}t} = \frac{\mathrm{d}(C(t)v(t))}{\mathrm{d}t} = C(t)\frac{\mathrm{d}v(t)}{\mathrm{d}t} + \frac{\mathrm{d}C(t)}{\mathrm{d}t}v(t)\,, \quad (14)$$

$$v(t) = \frac{\mathrm{d}\phi(t)}{\mathrm{d}t} = \frac{\mathrm{d}(L(t)i(t))}{\mathrm{d}t} = L(t)\frac{\mathrm{d}i(t)}{\mathrm{d}t} + \frac{\mathrm{d}L(t)}{\mathrm{d}t}i(t)\,, \quad (15)$$

for a capacitor and inductor respectively [22, p. 40, 47].

2.4. Generalized Time-Varying Models

We propose a generalized time-varying model of a lumped reactive element by incorporating the real parameter λ

$$i(t) = C^{1-\lambda}(t)\,\frac{\mathrm{d}}{\mathrm{d}t}\left(C^\lambda(t)\,v(t)\right), \qquad (16)$$

$$v(t) = L^{1-\lambda}(t)\,\frac{\mathrm{d}}{\mathrm{d}t}\left(L^\lambda(t)\,i(t)\right), \qquad (17)$$

for a capacitor and inductor respectively. These models include the circuit-theoretic model ($\lambda = 1$), Fettweis model ($\lambda = 1/2$) and traditional model ($\lambda = 0$) as special cases.

Looking at the instantaneous power $p(t) = v(t)i(t)$ for these two models, we obtain the following expressions

$$p_{C,\lambda}(t) = \frac{d}{dt}E_C(t) + 2E_C(t)\left(\lambda - \frac{1}{2}\right)\frac{1}{C(t)}\frac{dC}{dt}, \quad (18)$$

$$p_{L,\lambda}(t) = \frac{d}{dt}E_L(t) + 2E_L(t)\left(\lambda - \frac{1}{2}\right)\frac{1}{L(t)}\frac{dL}{dt}, \quad (19)$$

where $E_C(t) = C(t)v^2(t)/2$ and $E_L(t) = L(t)i^2(t)/2$ are the non-negative energies of the capacitor and the inductor. Note that the instantaneous power reduces to the derivative of the energy in the case of Fettweis ($\lambda = 1/2$) and thus it is lossless [21, 16].

3. DISCRETIZATION

Here we review traditional LTI discretization via the bilinear transform (BLT) and discretize our proposed models using the new α-transform discretization scheme. The results of these discretizations (24)–(43) are collected in Tab. 2 at the end of the paper.

The traditional way to discretize an element in WDF theory [4] involves first transforming its constitutive equation to the wave domain via (2) and then discretizing it using the BLT. Using this discretization on a capacitor yields (24) and on an inductor yields (34). The BLT is derived from the unidirectional Laplace transform, which assumes LTI and steady-state [23]. For most audio circuits, neither of these assumptions hold true and BLT discretization will cause errors.

Instead of using the BLT we use the α-transform discretization scheme [10, 8]. The α-transform discretization scheme is a generalization that encompasses the trapezoidal discretization scheme ($\alpha = 1$), backward-Euler ($\alpha = 0$) and forward-Euler ($\alpha \to \infty$) as special cases. Like trapezoidal integration, it does not depend on time-invariance or steady-state.

3.1. Discretizing the Generalized Model

To demonstrate how the α-transform discretization scheme is applied, we discretize our generalized capacitor model (16). Before we go into the general case we show how to apply the trapezoidal numerical scheme ($\alpha = 1$). As in traditional WDF theory we begin by applying (2) to transform (16) into the wave-domain

$$\frac{a_0(t) - b_0(t)}{R_0^\rho(t)C^{1-\lambda}(t)} = \frac{d}{dt}\left(\frac{a_0(t) + b_0(t)}{R_0^{\rho-1}(t)C^{-\lambda}(t)}\right). \quad (20)$$

Each side is now integrated over the time interval $[T(n-1), Tn]$, where T is the sampling period and n is the discrete-time sample index. The trapezoidal rule [24] is used to approximate the integrated expression on the left

$$\int_{T(n-1)}^{Tn} \frac{a_0(t) - b_0(t)}{R_0^\rho(t)C^{1-\lambda}(t)}\,dt$$
$$\approx \frac{T}{2}\left(\frac{a_0[n] - b_0[n]}{R_0^\rho[n]\,C^{1-\lambda}[n]} + \frac{a_0[n-1] - b_0[n-1]}{R_0^\rho[n-1]\,C^{1-\lambda}[n-1]}\right) \quad (21)$$

and the first fundamental theorem of calculus [25] to calculate the expression on the right over the same time interval

$$\int_{T(n-1)}^{Tn} \frac{d}{dt}\left(\frac{a_0(t) + b_0(t)}{R_0^{\rho-1}(t)C^{-\lambda}(t)}\right)\,dt$$
$$= \frac{a_0[n] + b_0[n]}{R_0^{\rho-1}[n]C^{-\lambda}[n]} - \frac{a_0[n-1] + b_0[n-1]}{R_0^{\rho-1}[n-1]C^{-\lambda}[n-1]}. \quad (22)$$

Combining (21) and (22) and solving for $b_0[n]$ gives us the multiplication coefficients shown in equation (32), for $\alpha = 1$. The multiplication coefficients for the BLT based capacitor is shown in (24). These two sets of multiplier coefficients differ with respect to time indices of the port resistance, and scaling of capacitance, not dissimilar to the results obtained in [26].

The generalized difference equation can be obtained by discretizing (20) using the α-transform discretization scheme. As shown in [10] a time-varying system of the form $\dot{x}(t) = y(x, t)$ may be discretized using the difference equation

$$(1 + \alpha)\,x[n] - (1 + \alpha)\,x[n - 1] = T\,y[n] + \alpha T\,y[n - 1] \quad (23)$$

Here $\dot{x}$ is the right-hand side of (20) and y is the left-hand side. Carrying this out and solving for $b_0[n]$ yields the multiplier coefficients (32). The inductor can be discretized using the same method, yielding the multiplier coefficients (42). Tab. 2 shows general discretizations, the three special cases (Traditional, Fettweis, and Time-Varying) and the LTI discretization, as well as the *adapted* ($R_0[n]$ chosen to set $n_0[n] = 0$) versions of each, for both the capacitor and the inductor.

4. CASE STUDY: TIME-VARYING RESISTANCES

In this section we simulate a simple series RC circuit involving a time-varying resistance. Depending on whether the capacitor is at the root of the WDF tree or not, this may cause simulation inaccuracies using the BLT. By discretizing the capacitor using an α-discretization, these inaccuracies are avoided.

In both cases, we allow the circuits to settle to a dc solution, change the value of a resistor, and examine the effect on the output variables under different discretization schemes [3]. In each case we analytically derive the dc solution of the WDF so that we can set initial conditions "at dc" without any wait.

4.1. Circuit Description

Consider the series RC circuit whose schematic is shown in Fig. 3a. In this circuit, an ideal voltage source v_{in}, resistor R_1, and capacitor C_1 are connected in series. The capacitor is characterized by voltage $v_{C,1}$ and current $i_{C,1}$. Taking v_{in} as the input and $v_{C,1}$ as the output of the circuit, it forms a first-order (6 dB/octave) low-pass filter with a cutoff frequency of

$$f_{cutoff} = 1/(2\pi R_1 C_1)\text{ Hz}. \quad (44)$$

Fig. 3b shows the series RC circuit decomposed into two one-port devices: the capacitor C_1 and a resistive voltage source composed of v_{in} and R_1. In such a simple circuit, the SPQR tree representing how the components are connected is trivial [27, 7]. However, this tree may be oriented in two different ways: with the resistive source at the root (Fig. 3c) or with C_1 at the root (Fig. 3d). These two tree orientations correspond to two different WDF diagrams: Figs. 3e and 3f respectively.

(a) *Schematic.*   (b) *Rearranged.*

root: $v_{\text{in}} \& R_1$ root: C_1

(c) *SPQR Tree (C_1 leaf).*   (d) *SPQR Tree (C_1 root).*

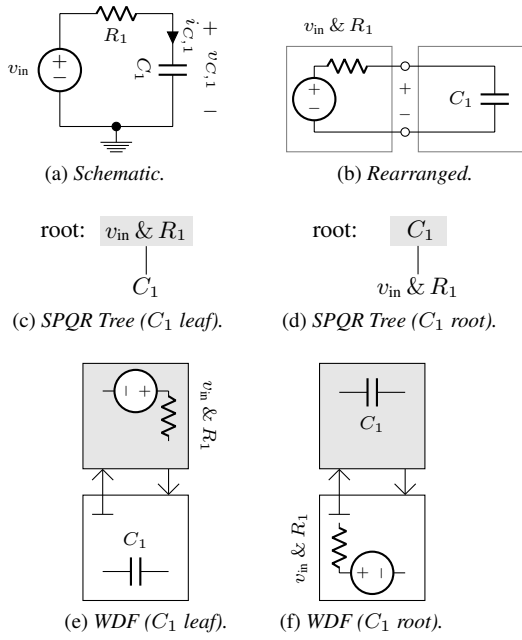(e) *WDF (C_1 leaf).*   (f) *WDF (C_1 root).*

Figure 3: *Series RC circuit schematic, decomposition into ports, two possible SPQR trees, and two corresponding WDF diagrams.*

The signal flow graphs corresponding to these WDFs use the same notation as before (as well as delays, z^{-1}) and are shown in Fig. 4. In each case the output variables are formed by (1)

$$v_{C,1} = R_0^{1-\rho}(a_{C,1} + b_{C,1})/2\,, \tag{45}$$

$$i_{C,1} = R_0^{-\rho}(a_{C,1} - b_{C,1})/2\,. \tag{46}$$

Note however that the port resistance R_0 and multipliers n_0, n_1, d_1, f, and g will be different. For example, n_1 in Fig. 4a and Fig. 4b are not the same. Port resistance and multiplier values will be given later as we test out the different discretization techniques.

4.1.1. Description of DC Behavior

In continuous time, the dc behavior (assuming $v_{\text{in}}(t) = 1\,\text{V}, \forall t < 0$) of the series RC circuit (Fig. 3a) is easy to predict. At dc, capacitors "look like" open circuits (they have "infinite" resistance at dc). Since no current may flow through C_1 at dc, no current may flow through R_1 either, so no voltage may develop across R_1. This leads to a dc solution for the capacitor network variables:

$$V_{C,1} = 1\,\text{V}, \quad (47) \qquad\qquad I_{C,1} = 0\,\text{A}. \quad (48)$$

Here and throughout, capital letters indicate dc quantities. In Fig. 5 a time-domain simulation of the circuit settling towards dc from zero initial conditions in response to the 1 V input is shown. Here and throughout, the sampling rate is $f_{\text{s}} = 44\,100\,\text{Hz}$.

4.1.2. Finding DC Solution of WDFs

We will use simple signal flow graph manipulation techniques [28, 29] to solve the dc solution of our simple WDFs.[1] First we recall a few elementary transformations on signal flow graphs:

---

[1] In general, for more complicated circuits, it could be more convenient to use matrix-based techniques [30] to find dc solutions.
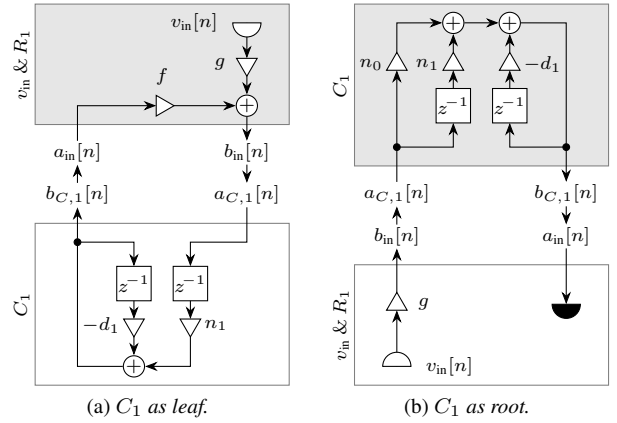

(a) C_1 *as leaf.*   (b) C_1 *as root.*

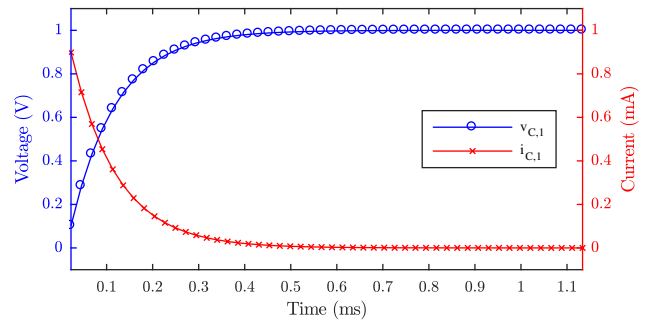Figure 4: *WDF signal flow graphs for different tree orientations.*

Figure 5: *RC circuit settling to dc. $R_1 = 1\,\text{k}\Omega$ and $C_1 = 0.1\,\mu\text{F}$.*

- Two multipliers χ and ζ in series may be replaced by a single multiplier $\chi\zeta$.
- Two multipliers χ and ζ in parallel may be replaced by a single multiplier $\chi + \zeta$.
- A self-loop though a multiplier χ may be replaced by a multiplier $1/(1 - \chi)$. This creates a singularity when $\chi = 1$.
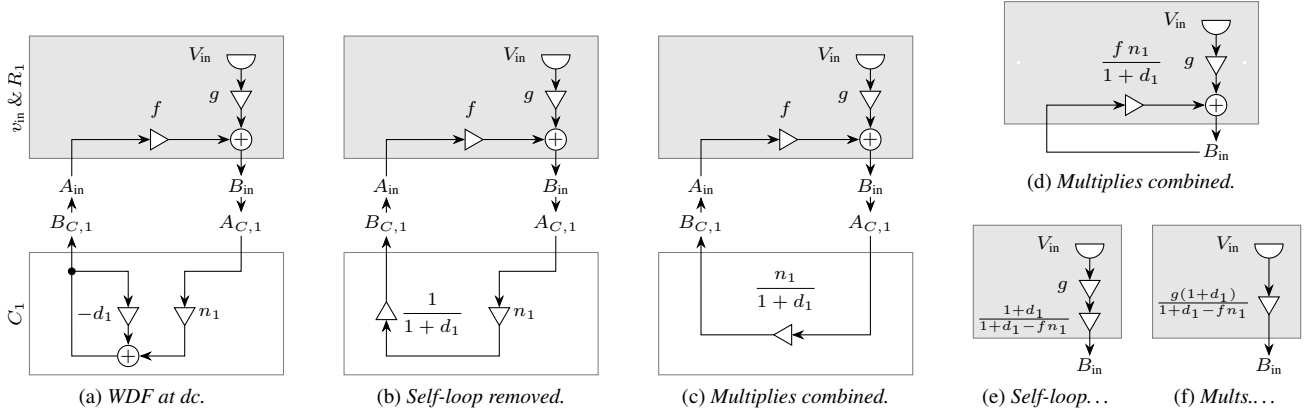
After a circuit has converged to dc, delays should be "transparent" so their outputs should equal their inputs, i.e., they can be replaced by a unity-gain, delay-free connection.

4.1.3. DC Solution with C_1 as Leaf

According to this logic, Fig. 4a at dc is shown in Fig. 6a. We see that a self-loop through $-d_1$ can be removed, giving Fig. 6b. Here the multiplier $1/(1 + d_1)$ and n_1 can be combined, giving Fig. 6c. Here the multipliers $n_1/(1 + d_1)$ and f can be combined, giving Fig. 6d. Here the self-loop through $fn_1/(1 + d_1)$ can be removed, giving Fig. 6e. Finally, the gains g and $(1 + d_1)/(1 + d_1 - fn_1)$ can be combined, giving Fig. 6f which solves for B_{in} in terms of V_{in}. This can be used to find the dc solution

$$A_{C,1} = B_{\text{in}} = \frac{g(1 + d_1)}{1 + d_1 - fn_1}V_{\text{in}} \tag{49}$$

$$A_{\text{in}} = B_{C,1} = \frac{n_1}{1 + d_1}A_{C,1} = \frac{g\,n_1}{1 + d_1 - fn_1}V_{\text{in}}\,. \tag{50}$$

(a) *WDF at dc.*   (b) *Self-loop removed.*   (c) *Multiplies combined.*   (d) *Multiplies combined.*   (e) *Self-loop...*   (f) *Mults....*

Figure 6: *Finding dc solution for series RC WDF with source at root and C_1 at leaf.*

(a) *WDF at dc.*   (b) *Multiplies combined.*   (c) *Self-loop removed.*   (d) *Multiplies combined.*
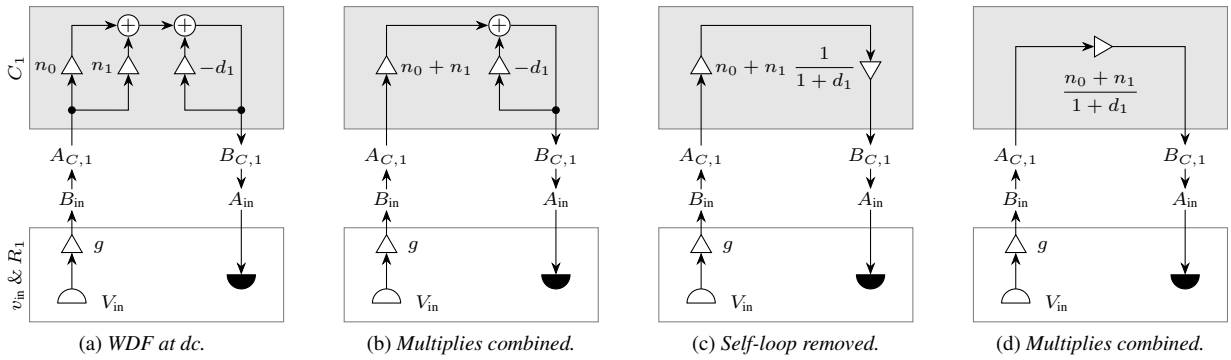
Figure 7: *Finding dc solution for series RC WDF with C_1 at root and source at leaf.*

Notice that $n_1/(1 + d_1) = 1$. Recall that $B_{C,1}$ and $A_{C,1}$ are also the values stored in the two delays. That is, they are the specific values that should be stored in those delays to set up the WDF as if it has converged to steady-state. These quantities are combined using (2) to find the dc solution for the network in terms of the WDF multipliers and input:

$$V_{C,1} = \frac{g(1 + d_1 + n_1)R_0^{1-\rho}}{2(1 + d_1 - fn_1)}V_{\text{in}} \qquad (51)$$

$$I_{C,1} = \frac{g(1 + d_1 - n_1)R_0^{-\rho}}{2(1 + d_1 - fn_1)}V_{\text{in}}. \qquad (52)$$

Now we can check these values, making sure that they correspond to the continuous-time steady-state solution (47)–(48). This is done by plugging in the values for the multipliers from each discretization (see Tab. 2). We will do this in the general case only, since when R_1 and C_1 are not changing (remember we are finding a steady-state solution) then it can encompass all the other discretizations mentioned, including the LTI ones.

Plugging in the multiplier values from the adapted generalized model (33), the unadapted resistive voltage source (Tab. 1) and circuit input values (51)–(52)

$$V_{\text{in}} = 1\,\text{V} \qquad\qquad g = 2R_0^\rho/(R_1 + R_0)$$
$$R_0 = T/(C_1(1 + \alpha)) \qquad n_1 = (\alpha + 1)/2$$
$$f = (R_1 - R_0)/(R_1 + R_0) \qquad d_1 = (\alpha - 1)/2$$

yields the the dc wave solutions

$$A_{C,1} = B_{\text{in}} = A_{\text{in}} = B_{C,1} = R_0^{\rho-1}. \qquad (53)$$

combining these solutions and the wave definition (2) yields the dc Kirchhoff solution

$$V_{C,1} = 1\,\text{V} \qquad (54) \qquad\qquad I_{C,1} = 0\,\text{A}. \qquad (55)$$

This matches the continuous-time dc solution (47)–(48), which is expected because the entire family of α-discretizations (except the degenerate $\alpha = -1$) should be consistent (for the LTI versions, dc is matched). As a sanity check we can run a simulation for a long time (many times longer than the time constant of the circuit) to confirm both the wave-domain (53) and Kirchhoff-domain dc solutions (51)–(52).

4.1.4. DC Solution with C_1 as Root

Fig. 4b at dc is shown in Fig. 7a. We see that the parallel multipliers n_0 and n_1 can be combined, giving Fig. 7b. Here the self loop through $-d_1$ can be removed, giving Fig. 7c. Finally, the series multipliers $n_0 + n_1$ and $1/(1 + d_1)$ can be combined, giving Fig. 7d which solves for the dc wave variables:

$$A_{C,1} = B_{\text{in}} = g\,V_{\text{in}}, \qquad (56)$$

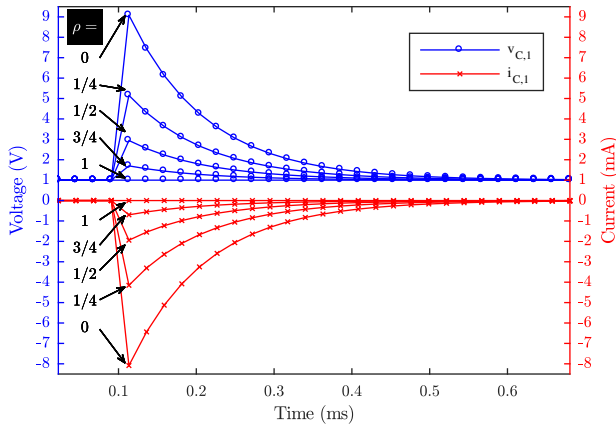$$A_{\text{in}} = B_{C,1} = \frac{n_0 + n_1}{1 + d_1}A_{C,1}. \qquad (57)$$

Figure 8: *Changing R_1 after 5 samples with various $\rho \in \{0, 1/4, 1/2, 3/4, 1\}$. C_1 at root of WDF tree. $\alpha = 1$.*
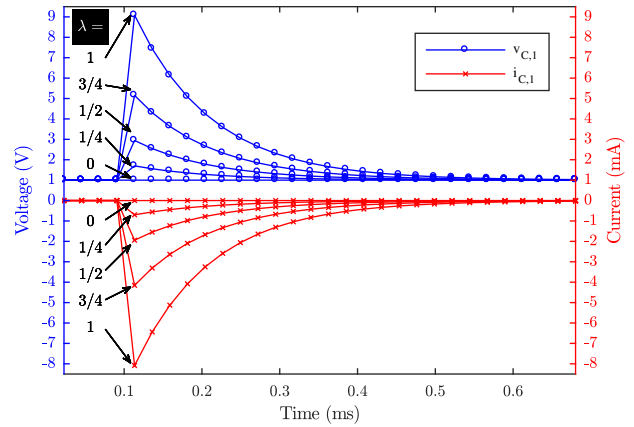

Figure 9: *Changing C_1 after 5 samples with various $\lambda \in \{0, 1/4, 1/2, 3/4, 1\}$. $\alpha = 1$ and $\rho = 1$.*

Notice that $(n_0 + n_1)/(1 + d_1) = 1$. These quantities are combined using (2) to find the dc solution for the network in terms of the WDF multipiers and input

$$V_{C,1} = \frac{(1 + n_0 + n_1)R_0^{1-\rho}}{2(1 + d_1)} V_{\text{in}}, \tag{58}$$

$$I_{C,1} = \frac{(1 - n_0 + n_1)R_0^{-\rho}}{2(1 + d_1)} V_{\text{in}}. \tag{59}$$

Plugging in the multiplier values for the adapted resistive source (Tab. 1) and discretized capacitor (32) as before

$$V_{\text{in}} = 1\,\text{V} \qquad n_0 = (T - (1 + \alpha)R_0 C_1)/(T + (1 + \alpha)R_0 C_1)$$
$$R_0 = R_1 \qquad n_1 = (T\alpha + (1 + \alpha)R_0 C_1)/(T + (1 + \alpha)R_0 C_1)$$
$$g = R_1^{\rho-1} \qquad d_1 = (T\alpha - (1 + \alpha)R_0 C_1)/(T + (1 + \alpha)R_0 C_1)$$

yields the dc wave solutions

$$A_{C,1} = B_{\text{in}} = A_{\text{in}} = B_{C,1} = R_1^{\rho-1}. \tag{60}$$

Note again that $B_{C,1}$ and $A_{C,1}$ are the values to be stored in the two delays. Combining (60) and the wave definition (2) yields the dc Kirchhoff solution

$$V_{C,1} = 1\,\text{V} \qquad (61) \qquad\qquad I_{C,1} = 0\,\text{A}. \qquad (62)$$

Again this matches the continuous-time dc solution (47)–(48) and sanity check simulations also confirm this.

4.1.5. Time-Varying Simulations

We now run a simulation of the series RC circuit with time-varying resistor values. In this simulation, the resistor and capacitor values vary as a function of the sample index n according to

$$R_1[n] = \begin{cases} 100\,\Omega, & n < 5 \\ 1\,\text{k}\Omega, & n \geq 5 \end{cases} \quad (63) \qquad C_1[n] = 0.1\,\mu\text{F}. \quad (64)$$

Recalling the equation for the filter's cutoff frequency (44), this circuit acts as a filter whose cutoff frequency varies with time

$$f_{\text{cutoff}} \approx \begin{cases} 15.9\,\text{kHz}, & n < 5 \\ 1.59\,\text{kHz}, & n \geq 5 \end{cases}. \tag{65}$$

WDF simulations of this circuit are made using the computational strutures in Fig. 4, using BLT discretizations and the generalized discretizations (with $\alpha = 1$). Because the capacitance does not change over time, the value of λ does not matter. We start the simulations at their dc solutions as calculated in the previous section. That is, the delay registers are loaded at $n = 0$ with the appropriate wave dc solutions (53) or (60).

For the case where C_1 is the leaf of the tree (Fig. 4b), there are no errors for any values of ρ for either the BLT or the generalized discretization. This can be explained by comparing (25) and (27), which are equivalent when the capacitor's value is static. Surprisingly, even though the BLT discretization should not be valid for time-varying circuits, it is acceptable for all values of ρ when C_1 is a leaf. The generalized transform, for all values of α and λ, has no errors since it has been discretized correctly.

In Fig. 8 simulations are shown using BLT discretizations (24) for the case where C_1 is the root of the tree (Fig. 4b). For voltage-wave BLT discretization ($\rho = 1$) we get the correct response, but for BLT discretization for any other ρ there are spurious transients. This discrepancy can be explained by comparing (24) and (26). Even for a static capacitor value, the BLT does not match the trapezoidal rule for the n_1 and d_1 coefficients except for the case $\rho = 1$ (voltage waves). Notice that for the inductor equations, this property would only hold for $\rho = 0$ (current waves).

5. CASE STUDY: TIME-VARYING REACTANCES

Now we study the series RC circuit with a time-varying capacitor value. In this simulation, the capacitor value vary as a function of the sample index n according to

$$R_1[n] = 1\,\text{k}\Omega \quad (66) \qquad C_1[n] = \begin{cases} 1.0\,\mu\text{F}, & n < 5 \\ 0.1\,\mu\text{F}, & n \geq 5 \end{cases}. \quad (67)$$

Recalling the equation for the filter's cutoff frequency (44), this circuit acts as a filter whose cutoff frequency varies as

$$f_{\text{cutoff}} \approx \begin{cases} 0.159\,\text{kHz}, & n < 5 \\ 1.59\,\text{kHz}, & n \geq 5 \end{cases}. \tag{68}$$

WDF simulations of this circuits are made using the computational structures in Fig. 4, using the generalized discretization

(with $\alpha = 1$). Again we assume that the simulation has converged to a dc solutions (53) or (60) by time $n = 0$.

For both cases, where C_1 is the root of the tree (Fig. 2b) or the leaf of the tree (Fig. 2b), Fig. 9 shows simulations using (32) or (33). Since the generalized discretization is used correctly, there is no difference in behavior between the two configurations. By varying λ a family of responses are obtained. For $\lambda = 0$ (traditional model), there is no transient, i.e., the capacitor's state is maintained under time-varying conditions. For $\lambda = 1/2$ (Fettweis model), the energy is maintained but there *is* a transient. For $\lambda = 1$ (time-varying circuit theory model), the transient is the largest. We cannot necessarily say that one behavior is intrinsically the best; the appropriate choice of λ will depend on the desired behavior.

6. CONCLUSIONS

In this paper we argue for the use of proper numerical schemes since the theory that lies at the foundation of the discretization methods used in WDFs is invalid under time-varying conditions. Numerical schemes like the α-transform discretization and trapezoidal rule, however, have no problems with time-varying systems when applied properly.

If your goal is to model LTI circuits, traditional bilinear transform based discretizations generally suffice. In the case where a reactance is placed at the root of a tree but other elements may change its port resistance, you should discretize it using the trapezoidal method in order to avoid inaccuracies in the simulation.

When faced with the problem of simulating time-varying reactances we would recommend to gather data and use any number of optimization methods to get an estimate for a suitable value of λ. For some circuits the effects caused by time-varying reactances make up an important part of the sound, such as is the case with stepped filters, or even the intrinsic operation of the device, e.g. condenser microphone. Conversely in other cases the "smoothness" and/or reduction of transient may be a desired behavior. In any case, the parameter λ in our proposed continuous-time model allows the algorithm designer to control the behavior.

In closing, the combination of the novel generalized continuous-time capacitor and inductor models, α-discretizations, and parametric wave definition gives new tools that may be useful when creating audio effects and gives audio dsp designers more control over how energy is stored in discretized reactances.

7. REFERENCES

[1] S. Bilbao, "Time-varying generalizations of allpass filters," *IEEE Signal Process. Lett.*, vol. 12, no. 5, pp. 376–379, May 2005.

[2] J. Laroche, "On the stability of time-varying recursive filters," *J. Audio Eng. Soc. (JAES)*, vol. 55, no. 6, pp. 460–471, June 2007.

[3] A. Wishnick, "Time-varying filters for musical applications," in *Proc. 17th Int. Conf. Digital Audio Effects (DAFx-14)*, Erlangen, Germany, Sept. 2014, pp. 69–76.

[4] A. Fettweis, "Wave digital filters: Theory and practice," *Proc. IEEE*, vol. 74, no. 2, pp. 270–327, Feb. 1986.

[5] K. J. Werner, J. O. Smith III, and J. S. Abel, "Wave digital filter adaptors for arbitrary topologies and multiport linear elements," in *Proc. 18th Int. Conf. Digital Audio Effects (DAFx-15)*, Trondheim, Norway, Nov. 2015, pp. 379–386.

[6] K. J. Werner, V. Nangia, J. O. Smith III, and J. S. Abel, "Resolving wave digital filters with multiple/multiport nonlinearities," in *Proc. 18th Int. Conf. Digital Audio Effects (DAFx-15)*, Trondheim, Norway, Nov. 2015, pp. 387–394.

[7] K. J. Werner, A. Bernardini, J. O. Smith III, and A. Sarti, "Modeling circuits with arbitrary topologies and active linear multiports using wave digital filters," *IEEE Trans. Circuits. Syst. I: Reg. Papers*, June 2018, In Press, DOI: 10.1109/TCSI.2018.2837912.

[8] K. J. Werner, *Virtual Analog Modeling of Audio Circuitry Using Wave Digital Filters*, Ph.D. diss., Stanford Univ., CA, USA, Dec. 2016.

[9] A. Bernardini and A. Sarti, "Biparametric wave digital filters," *IEEE Trans. Circuits Syst. I: Reg. Papers*, vol. 64, no. 7, pp. 1826–1838, July 2017.

[10] F. G. Germain and K. J. Werner, "Design principles for lumped model discretisation using Möbius transforms," in *Proc. 18th Int. Conf. Digital Audio Effects (DAFx-15)*, Trondheim, Norway, November 2015, pp. 371–378.

[11] D. Fränken and K. Ochs, "Synthesis and design of passive Runge-Kutta methods," *Int. J. Electron. Commun. (AEÜ)*, vol. 55, no. 6, pp. 417–425, 2001.

[12] Ó. Bogason, "Modeling audio circuits containing typical nonlinear components with wave digital filters," M.A. thesis, McGill Univ., May 2018.

[13] H. W. Strube, "Time-varying wave digital filters for modeling analog systems," *IEEE Trans. Acoust., Speech, Signal Process.*, vol. 30, no. 6, pp. 864–868, Dec. 1982.

[14] H. W. Strube, "Time-varying wave digital filters and vocal-tract models," in *IEEE Int. Conf. Acoust., Speech, Signal Process. (ICASSP)*, May 1982, vol. 7, pp. 923–926.

[15] G. Kubin, "On the stability of wave digital filters with time-varying coefficients," in *Proc. 7th Europ. Conf. Circuit Theory Design (ECCTD-85)*, Prague, Czecho-Slovakia, Sept. 1985, pp. 499–502.

[16] S. Bilbao, *Wave and Scattering Methods for Numerical Simulation*, John Wiley and Sons, Ltd, New York, 2004.

[17] D. Fränken and K. Ochs, "Automatic step-size control in wave digital simulation using passive numerical integration methods," *Int. J. Electron. Commun. (AEÜ)*, vol. 58, pp. 391–401, 2004.

[18] M. J. Olsen, K. J. Werner, and F. G. Germain, "Network variable preserving step-size control in wave digital filters," in *Proc. 20th Int. Conf. Digital Audio Effects (DAFx-17)*, Edinburgh, UK, Sept. 2017, pp. 207–207.

[19] J. O. Smith, *Introduction to Digital Filters with Audio Applications*, W3K Publishing, https://ccrma.stanford.edu/ jos/filters/, 2007.

[20] T. S. Stilson, *Efficiently-Variable Non-Oversampled Algorithms in Virtual-Analog Music Synthesis—A Root-Locus Perspective*, Ph.D. diss., Stanford Univ., California, USA, June 2006.

[21] A. Fettweis, "Robust numerical integration using wave digital concepts," in *Proc. 5th DSPS Educators Conf.*, Tokyo, Japan, Sept. 2003, pp. 23–32.

[22] C. A. Desoer and E. S. Kuh, *Basic Circuit Theory*, McGraw-Hill, New York, NY, USA, 1969.

[23] M. Vetterli, J. Kovačević, and V. K. Goyal, *Foundations of Signal Processing*, Cambridge Univ. Press, 2014, Online: http://fourierandwavelets.org/.

[24] M. Parviz, *Fundamentals of Engineering Numerical Analysis*, Cambridge Univ. Press, Cambridge, UK, 2nd edition, 2010.

[25] A. Howard, *Calculus: A New Horizon*, Wiley, New York, NY, USA, 6th edition, 1998.

[26] J. S. Abel and D. P. Berners, "The time-varying bilinear transform," in *Proc. 141st Conv. Audio Eng. Soc. (AES)*, Los Angeles, CA, Sept. 2016, pp. 9686–9697, conv. paper #9686.

[27] D. Fränken, J. Ochs, and K. Ochs, "Generation of wave digital structures for networks containing multiport elements," *IEEE Trans. Circuits Syst. I, Reg. Papers*, vol. 52, no. 3, pp. 586–596, Mar. 2005.

[28] S. J. Mason, "Feedback theory—further properties of signal flow graphs," *Proc. IRE*, vol. 44, no. 7, pp. 920–926, July 1956.

[29] K. J. Werner, J. S. Abel, and J. O. Smith, "More cowbell: a physically-informed, circuit-bendable, digital model of the TR-808 cowbell," in *Proc. 137th Conv. Audio Eng. Soc. (AES)*, Los Angeles, CA, USA, Oct. 2014, conv. paper #9207.

[30] A. Sarti and G. De Sanctis, "Systematic methods for the implementation of nonlinear wave-digital structures," *IEEE Trans. Circuits Syst. I: Reg. Papers*, vol. 56, no. 2, pp. 460–472, Feb. 2009.

(a) Capacitor discretizations and coefficients.

Eqn.	Model	Discret. Adapted?	n_0	n_1	d_1
(24)	LTI	BLT, No	$\frac{T-2R_0[n]C[n]}{T+2R_0[n]C[n]}$	1	$\frac{T-2R_0[n]C[n]}{T+2R_0[n]C[n]}$
(25)	LTI	BLT, $R_0[n]=\frac{T}{2C[n]}$	0	1	0
(26)	Traditional	Trap., No	$\frac{T-2R_0[n]C[n]}{T+2R_0[n]C[n]}$	$\frac{T+2R_0[n-1]C[n-1]}{T+2R_0[n]C[n]}\left(\frac{R_0[n]}{R_0[n-1]}\right)^\rho\left(\frac{C[n]}{C[n-1]}\right)^{1-\rho}$	0
(27)	Traditional	Trap., $R_0[n]=\frac{T}{2C[n]}$	0	$\left(\frac{C[n]}{C[n-1]}\right)^{1-\rho}$	0
(28)	Fettweis	Trap., No	$\frac{T-2R_0[n]C[n]}{T+2R_0[n]C[n]}$	$\frac{T+2R_0[n-1]C[n-1]}{T+2R_0[n]C[n]}\left(\frac{R_0[n]}{R_0[n-1]}\right)^\rho\sqrt{\frac{C[n]}{C[n-1]}}$	0
(29)	Fettweis	Trap., $R_0[n]=\frac{T}{2C[n]}$	0	$\left(\frac{C[n]}{C[n-1]}\right)^\rho\sqrt{\frac{C[n]}{C[n-1]}}$	0
(30)	Time-Varying	Trap., No	$\frac{T-2R_0[n]C[n]}{T+2R_0[n]C[n]}$	$\frac{T-2R_0[n-1]C[n-1]}{T+2R_0[n]C[n]}\left(\frac{R_0[n]}{R_0[n-1]}\right)^\rho$	0
(31)	Time-Varying	Trap., $R_0[n]=\frac{T}{2C[n]}$	0	$\left(\frac{C[n]}{C[n-1]}\right)^{-\rho}$	0
(32)	Generalized	α, No	$\frac{T-(1+\alpha)R_0[n]C[n]}{T+(1+\alpha)R_0[n]C[n]}$	$\frac{T\alpha+(1+\alpha)R_0[n-1]C[n-1]}{T+(1+\alpha)R_0[n]C[n]}\left(\frac{R_0[n]}{R_0[n-1]}\right)^\rho\left(\frac{C[n]}{C[n-1]}\right)^{1-\rho-\lambda}(1+\alpha)$	$\frac{T\alpha-(1+\alpha)R_0[n-1]C[n-1]}{T+(1+\alpha)R_0[n]C[n]}\left(\frac{R_0[n]}{R_0[n-1]}\right)^\rho\left(\frac{C[n]}{C[n-1]}\right)^{1-\rho-\lambda}(1-\alpha)$
(33)	Generalized	α, $R_0[n]=\frac{T}{(1+\alpha)C[n]}$	0	$\frac{1}{2}\left(\frac{C[n]}{C[n-1]}\right)^{1-\rho-\lambda}(1+\alpha)$	$-\frac{1}{2}\left(\frac{C[n]}{C[n-1]}\right)^{1-\rho-\lambda}(1-\alpha)$

(b) Inductor discretizations and coefficients.

Eqn.	Model	Discret. Adapted?	n_0	n_1	d_1
(34)	LTI	BLT, No	$\frac{2L[n]-TR_0[n]}{2L[n]+TR_0[n]}$	-1	$-\frac{2L[n]-TR_0[n]}{2L[n]+TR_0[n]}$
(35)	LTI	BLT, $R_0[n]=\frac{2L[n]}{T}$	0	-1	0
(36)	Traditional	Trap., No	$\frac{2L[n]-TR_0[n]}{2L[n]+TR_0[n]}$	$-\frac{2L[n-1]-TR_0[n-1]}{2L[n]+TR_0[n]}\left(\frac{R_0[n]}{R_0[n-1]}\right)^\rho\left(\frac{L[n]}{L[n-1]}\right)$	0
(37)	Traditional	Trap., $R_0[n]=\frac{2L[n]}{T}$	0	$-\left(\frac{L[n]}{L[n-1]}\right)^\rho$	0
(38)	Fettweis	Trap., No	$\frac{2L[n]-TR_0[n]}{2L[n]+TR_0[n]}$	$-\frac{2L[n-1]+TR_0[n-1]}{2L[n]+TR_0[n]}\left(\frac{R_0[n]}{R_0[n-1]}\right)^\rho\sqrt{\frac{L[n]}{L[n-1]}}$	0
(39)	Fettweis	Trap., $R_0[n]=\frac{2L[n]}{T}$	0	$-\left(\frac{L[n]}{L[n-1]}\right)^\rho\sqrt{\frac{L[n]}{L[n-1]}}$	0
(40)	Time-Varying	Trap., No	$\frac{2L[n]-TR_0[n]}{2L[n]+TR_0[n]}$	$-\frac{2L[n-1]-TR_0[n-1]}{2L[n]+TR_0[n]}\left(\frac{R_0[n]}{R_0[n-1]}\right)^\rho$	0
(41)	Time-Varying	Trap., $R_0[n]=\frac{2L[n]}{T}$	0	$-\left(\frac{L[n]}{L[n-1]}\right)^{\rho-1}$	0
(42)	Generalized	α, No	$\frac{(1+\alpha)L[n]-TR_0[n]}{(1+\alpha)L[n]+TR_0[n]}$	$-\frac{(1+\alpha)L[n-1]+T\alpha R_0[n-1]}{(1+\alpha)L[n]+TR_0[n]}\left(\frac{R_0[n]}{R_0[n-1]}\right)^\rho\left(\frac{L[n]}{L[n-1]}\right)^{1-\lambda}$	$-\frac{(1+\alpha)L[n-1]-T\alpha R_0[n-1]}{(1+\alpha)L[n]+TR_0[n]}\left(\frac{R_0[n]}{R_0[n-1]}\right)^\rho\left(\frac{L[n]}{L[n-1]}\right)^{1-\lambda}$
(43)	Generalized	α, $R_0[n]=\frac{(1+\alpha)L[n]}{T}$	0	$-\frac{1}{2}\left(\frac{L[n]}{L[n-1]}\right)^{\rho-\lambda}(1+\alpha)$	$-\frac{1}{2}\left(\frac{L[n]}{L[n-1]}\right)^{\rho-\lambda}(1-\alpha)$

Table 2: *Summary of inductor and capacitor discretizations and difference equation coefficients.*